SPACE-BASED RADIATION SIMULATIONS FOR INTERPRETATION OF AEROSOL EVENTS

Takuma Yokomae, Sonoyo Mukai, Itaru Sano and Makiko Nakata

Kinki University, Fac. of Sci & Tech, 3-4-1 Kowakae, Higashi-Osaka 577-8502, Japan

KEY WORDS: aerosol events, satellite data, radiative transfer, model simulation

ABSTRACT:

Large scale aerosol events such as dust storm and biomass burning plume frequently occur due to the unstable climate and/or global warming tendency. It is known that large scale-forest fire damages the Earth environment as biomass burning and emission of carbonaceous particles. It is also known that the heavy soil dust is transported from the China continent to Japan on westerly winds, and provides us with severe damages on the social life and/or human health. It is very difficult to do the sun/sky photometry of the Earth atmosphere from the ground in the case of aerosol events though, the satellite works well. Accordingly, the detection of such aerosol events as dust storm or biomass burning plume with multispectral satellite data is desired. Here the retrieval algorithms for aerosol events are examined based on new code of the radiative transfer for semi-infinite atmosphere model. The derived space-based results are compared with the model simulations. In this work, the space-/surface-based measurements, multiple scattering calculations and model simulations are combined together for remote sensing of aerosol events.

1. INTRODUCTION

It is well known that atmospheric aerosols play an important role in the Earth's environments and global climate changes, and also provide the sufficient influences upon the human activates. Thus precise retriecal of the atmospheric aerosol is an urgent subject.

Our research group have been working to retrieve aerosol characteristics with combination use of satellite data and ground measurements (Mukai 1990, Sano et al. 2010), and numerical model simulations (Nakata et al. 2004).

In this study, we focus on the large scale aerosol events, which indicate too much loading of aerosols, with in the atmosphere, such as dust storm and biomass burning. In the middle of aerosol events, it is hard to work the ground-based measurements such as sun/sky photometry. However, the satellites are available to observe the spectral radiance reflected from the atmosphere model is developed in order to retrieve the aerosol properties in the aerosol events (Sano et al. 2009). The radiation field reflected from the optically semi-infinite atmosphere model is descried with the successive order of scattering method (Uesugi et al.1970; Mukai et al. 1979)

2. ALGORITHM FOR AEROSOL RETRIEVAL

Figure 1 shows a block flow for aerosol retrieval which is divided into three parts as: satellite data analysis (S), model simulations (M) and radiative transfer calculations (R). The aerosol properties such as aerosol optical thickness (AOT), refractive index (m) and angstrom exponential (α) are estimated by comparing satellite measurements with the numerical values of radiation simulations in the Earth-atmosphere-surface model. The model of the Earth's atmosphere is based on the AFGL-code, which provides us with the aerosol and molecular distribution with height (Kneizys 1988). In the multiple scattering calculations at part (R), Rayleigh scattering by molecules and Mie scattering by aerosols in the atmosphere are taken into account. The aerosol models are estimated from NASA/AERONET measurements (Holben 1998).

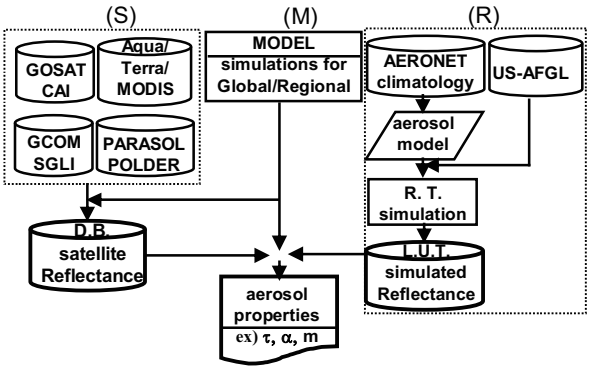

Figure 1. A block blow for aerosol retrieval

Our satellite database involves various types of space-based measurements as much as possible for our usage. For examples, MODIS sensor mounted on the satellite Terra and Aqua, and GLI (GLobal Imager) on the satellite ADEOS-2 measure the spectral radiance at top of the atmosphere (TOA) from visible to far infrared wavelengths, POLDER sensor on ADEOS and PARASOL provides us with the polarization information, and GOSAT/CAI has a ultraviolet wavelength band. These space borne sensors measure the upwelling radiance at the top of atmosphere, and hence the satellite data involve the radiance due to both of atmospheric scattering and ground surface reflection. It is known in the satellite data analysis that the separation of atmospheric information from ground-surface one is very difficult. It is very difficult to do the sun/sky photometry of the Earth atmosphere from the ground in the

case of aerosol events though, the satellite works well. Accordingly, the detection of such aerosol events as dust storm or biomass burning plume with multispectral satellite data is desired. Here the retrieval algorithms for aerosol events are examined based on new code of the radiative transfer for semi-infinite atmosphere model. The derived space-based results are compared with the model simulations. In this work, the space-/surface-based measurements, multiple scattering calculations and model simulations are combined together for remote sensing of aerosol events.

3. RADIATION SIMULATIONS FOR AEROSOL EVENTS

3.1 Aerosol Events

The large scale aerosol events are frequency caused by the unstable climate and/or global warming tendency, and cause serious influence on the Earth's environment and the social life. For example, the large scale-forest fire is generated too much biomass burning aerosols. It is also known that the heavy soil dust, called yellow sand, is transported from China continent to Japan on westerly winds especially in spring. Aerosol events influence to the Earth's environment, the social life and human health.

Figure 2 presents simple illustration of the Earth atmosphere composed of gas molecules and aerosols, which are denoted by black dots and gray circles, respectively, and aerosol optical thickness (AOT) is represented by τ. Increasing the amount of aerosol particles in the atmosphere, AOT becomes higher as shown in Figure 2. In the aerosol events, aerosols are overloading in the atmosphere, namely AOT takes semi-infinite value in the extreme case. In such a case it is very difficult to observe atmospheric aerosols from the ground surface.

On the contrary, the satellite works well due to observe the Earth atmosphere from the space. The Asian dust storm is detected by using visible and near infra-red spectral data by MODIS (Mukai et al. 2010). And biomass burning aerosols are also detected based on the ratio of reflectance at a wave length of 0.412μm to that at 0.38 μm given by ADEOS-2/GLI (Sano 2009).

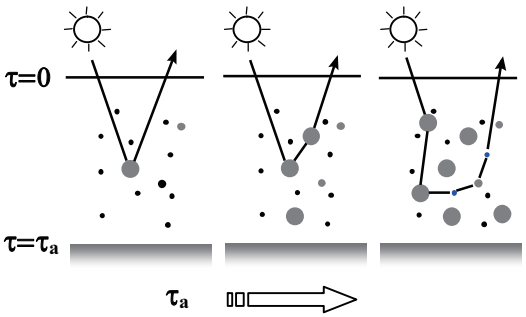

Figure 2. Illustration of atmospheric model composed of gas molecules and aerosols represented by black dots and gray circles, respectively, and τ_a denotes the aerosol optical thickness of the atmosphere.

3.2 Radiative Transfer Equation

Here, radiation simulation in the case of aerosol event is treated with the semi-infinite atmosphere model. The successive order of scattering method is employed (Uesugi et al. 1970). The incident sun light at the top of atmosphere (TOA) is scattered many times with the gas molecules and/or aerosols in the Earth atmosphere (see Figure 2).

The specific intensity of radiation $I(\tau, \Omega)$ at optical depth τ in the atmosphere with direction Ω is expressed by the radiative transfer equation (Chandrasekhar, 1960) as:

$$\mu[dI(\tau,\Omega)/d\tau] = I(\tau,\Omega)-(\varpi/4\pi) \times \int P(\Omega, \Omega') I(\tau, \Omega') d\Omega'. \quad (1)$$

where ϖ is the albedo for single scattering and $P(\Omega,\Omega')$ represents the phase function for single scattering $P(\Omega,\Omega')$. The solid angles Ω and Ω' represent the directions of propagation and incident, which are written by zenith angle (θ) and azimuth angle (φ). Note that the cosine of zenith angel ($\mu=\cos\theta$) is available in usual. Thus the scattering angle (Θ) for single scattering process is expressed as follows:

$$\cos\Theta = \mu\mu' + (1-\mu)^{1/2}(1-\mu'^2)^{1/2}\cos(\varphi-\varphi'). \quad (2)$$

Therefore, the phase function $P(\Omega, \Omega_0)$ are written by $P(\mu, \mu_0; \varphi-\varphi_0)$, which can be expanded in Fourier series with respect to $\varphi-\varphi_0$ for efficient calculations (Mukai, 1979),

$$P(\Omega, \Omega_0) = P^{(0)}(\mu, \mu^0) + + 2\sum_{i=1}^{\infty} [\ P_c^{(i)}(\mu, \mu_0)\cos i \times (\varphi-\varphi_0) + + P_s^{(i)}(\mu, \mu_0)\sin i \times(\varphi-\varphi_0)\ ]. \quad (3)$$

3.3 Successive Order of Scattering

To solve the radiative transfer equation in eq.(1), various methods have been proposed. For example, the doubling method (Hansen, 1974) is based on the duplication of thin atmosphere. In the semi-infinite atmosphere case, many times of duplication process are needed. Naturally this fact is not practical. Then, successive order of scattering method is adopted for the present work. Assuming parallel radiation of net flux πF is incident at TOA with the specified direction $-\Omega_0$ as $(-\mu_0, \varphi_0)$. The reflected intensity at TOA is defined as:

$$I(0, +\Omega) = (\mu_0/4)R(\Omega,\Omega_0)\mathrm{F}, \quad (4)$$

where the F is the incident flux; we assume that the parallel beam of radiation of net flux πF is incident at the top of plane parallel atmosphere into some specified direction $-\Omega_0$ which can be written as $(-\mu_0, \varphi_0)$. $R(\Omega,\Omega_0)$ is a reflection function

for the emergent intensity at the top of the atmosphere (which equals $(\mu\mu_0)^{-1}S$, where S is a scattering function of Chandrasekhar (1960)). In the Successive Order of Scattering method, the $R(\Omega,\Omega_0)$ is calculated in the form of infinite series as

$$R\,\Omega,\,\Omega_0) = \sum_{n=1}^{\infty} \varpi^n R(\mathrm{n},\,\Omega,\,\Omega_0)\,, \qquad (5)$$

where n is number of scattering, $R^*(\mathrm{n},\,\Omega,\,\Omega_0)$ is the nth-order of reflection function which means the emergent radiation at TOA after n-time scattering within the atmosphere. And hence, $R^*(n\,\Omega,\Omega_0)$ relates to the product of lower-order reflection function $R^*(n\text{-}1\,\Omega,\Omega_0)$ and single scattering phase function $P\,(\Omega,\Omega_0)$ as:

$$(\mu+\mu_0)R^*(1{:}\,\Omega,\Omega_0) = P\,(\Omega,\Omega_0), \qquad (6)$$

$$(\mu+\mu_0)R^*(2{:}\,\Omega,\Omega_0 = (\mu / 4\pi) \int_- R^*(1{:}\,\Omega,\,\Omega')\,P\,(\Omega',\,\Omega_0)\,d\Omega' + + (\mu_0 / 4\pi\,) \int_+ P\,(\Omega,\,\Omega')\,R^*(1{:}\,\Omega',\,\Omega_0)\,d\Omega', \qquad (7)$$

$$(\mu+\mu_0)R^*(\mathrm{n}{:}\,\Omega,\Omega_0) = (\mu / 4\pi) \int_- R^*(\mathrm{n}\text{-}1{:}\,\Omega,\,\Omega')\,P\,(\Omega',\,\Omega_0)\,d\Omega' + + (\mu_0 / 4\pi\,) \int_+ P\,(\Omega,\,\Omega')\,R^*(\mathrm{n}\text{-}1{:}\,\Omega',\,\Omega_0)\,d\Omega' + + (\mu\mu_0/16\pi^2) \sum_{n'=1}^{n-2} \int_- R^*(\mathrm{n}\text{-}1{:}\,\Omega,\,\Omega')\;d\Omega'\times \times \int_+ P\,(\Omega',\,\Omega'')\,R^*(\mathrm{n}\text{-}1{:}\,\Omega'',\,\Omega_0)\,d\Omega'' \quad \text{for } \mathrm{n} \geq 3. \qquad (8)$$

The convergence of eq.(5) is very slow for ϖ nearly equal 1. In order to solve this problem, the following asymptotic form of $R^*(\mathrm{n})$ is proposed for higher-order of scattering.

$$R^*(\mathrm{n}{:}\,\Omega,\,\Omega_0) = A\mathrm{n}^{-3/2}\mathrm{e}^{-d/n} \qquad (9)$$

where the values of $A(\Omega,\,\Omega_0)$ and $d(\Omega,\,\Omega_0)$ are successively calculated and converging for large n. Employing of eq.(9) for total reflection function for n>n*>>1, eq.(5) becomes

$$R(\Omega,\Omega_0) = \sum_{n=1}^{n=n^*} \varpi^n R(\mathrm{n};\,\Omega,\,\Omega_0) + A \sum_{n=n^*+1}^{\infty} \varpi \mathrm{n}^{-3/2}\mathrm{e}^{-d/n} \qquad (10)$$

$$A(\Omega,\Omega_0) = R^*(1{:}\,\Omega,\,\Omega_0)\mathrm{n}^{*-3/2}\mathrm{e}^{d/n^*}\,. \qquad (11)$$

The second term of eq.(10) can be quickly calculated by using following transformation from summation to integration as:

$$\sum_{n=n^*+1}^{n=\infty} \varpi \mathrm{n}^{-3/2}\mathrm{e}^{-d/n} = \int_{n^*}^{\infty} dx\; x^{-3/2}\mathrm{e}^{-\alpha x} - d \int_{n^*}^{\infty} dx\; x^{-5/2}\,\mathrm{e}^{-\alpha x} \qquad (12)$$

where $\alpha = -\ln \varpi$. Accordingly, through integrating of eq.(12), eq.(10) can be write as:

$$R(\mathrm{n};\,\Omega,\Omega_0) = \sum_{n=1}^{n=n^*} \varpi^n R(\mathrm{n};\,\Omega,\,\Omega_0) + + 2A\mathrm{n}^{*-1/2}[\mathrm{e}^{-\alpha \mathrm{n}^*} - (\pi\alpha \mathrm{n}^*)^{1/2}\,\mathrm{erfc}(\sqrt{\alpha \mathrm{n}^*})] - - (2/3)\,Ad\mathrm{n}^{*-3/2}[(1 - 2\alpha \mathrm{n}^*)\mathrm{e}^{-\mathrm{an}^*} - - 2\pi^{1/2}(\alpha \mathrm{n}^*)^{3/2}\,\mathrm{erfc}(\sqrt{\alpha \mathrm{n}^*})]. \qquad (13)$$

where erfc(z) represents complementary error function.
The obtained asymptotic form of eq.(13) allows us to compute the total reflection function by using low-order of scattering alone.
It is interesting that this method of successive order of scattering provides us with the mean number of scattering,

$$\langle\, n\,(\Omega,\Omega_0)\,\rangle = = [\,\sum_{n=1}^{\infty} \mathrm{n}\, R^*(\mathrm{n};\,\Omega,\Omega_0)\,\varpi^n] \,/\, [\sum_{n=1}^{\infty} R^*(\mathrm{n};\,\Omega,\,\Omega_0)\,\varpi^n\,]. \qquad (14)$$

3.4 Numerical result

For the sake of validation of successive order of scattering method, a case of isotropic scattering (i.e. $P(\Theta)=1$) is examined with our new computational code. Figure 3 shows each order of scattering function ($R^*(\mathrm{n}{:}\,\Omega,\,\Omega_0)$) until n=150. It is found that higher-order of reflection functions converge into the asymptotic form expressed in eq.(9). Figure 4 presents the results of total reflection function $R(\Omega,\,\Omega_0)$. It is natural that total reflection converges with increasing the order of scattering due to small contribution of higher-order of scattering.

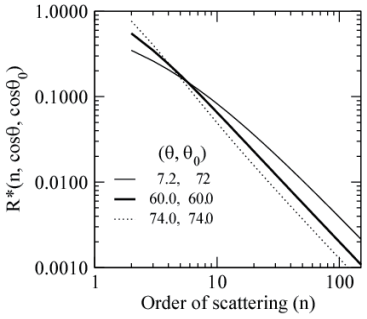

Figure 3. Result of reflection function of each order of scattering for isotropic scattering with ϖ=1.0.

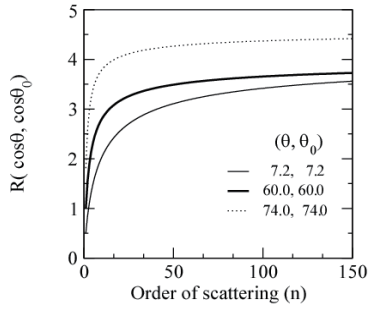

Figure 4. The same as Figure 3, but for total reflection function.

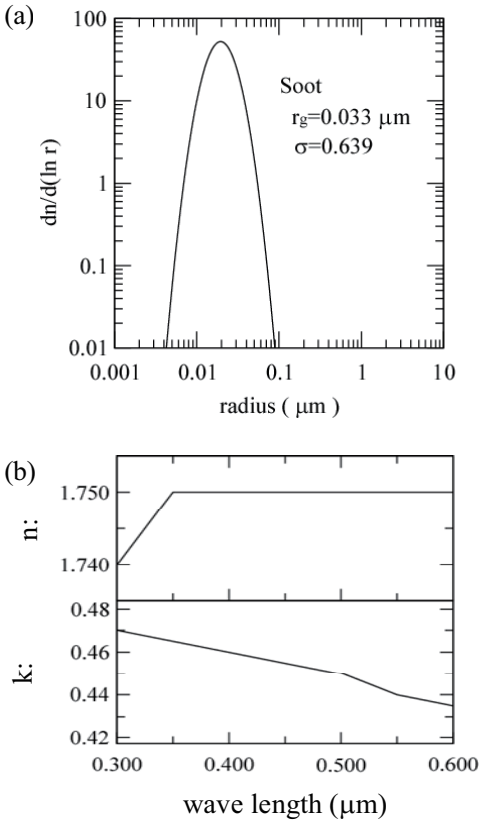

Figure 5. Size distribution function (a) and the values of refractive indices (b) for soot aerosol model.

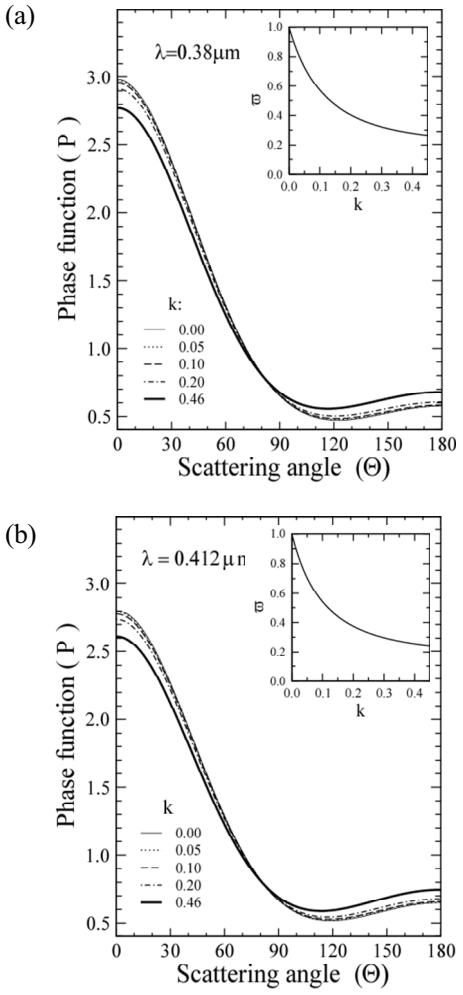

Figure 6. Phase function ($P(\Theta)$) and albedo for single scattering (ϖ) at wavelengths of 0.38mm (a) and 0.412mm (b) for aerosol models shown in figure 5.

4. DISCUSSION AND CONCLUSION

Figure 5 presents the characteristics of soot aerosol model. Figures 5a and 5b represent the lognormal size distribution, and the values of complex refractive indices (m=n-k*i*) with respect to the wavelength, respectively. The size distribution function is defined with r_g=0.033μm and σ=0.639, which denote the mean of geometric radius of particles and the standard deviation, respectively. It is shown from Figure 5 that the soot aerosols are small particles and strongly absorb the short wave length radiation. Figure 6 shows the numerical results of Mie calculation of phase function ($P(\Theta)$) and albedo (ϖ) for single scattering for soot aerosol models shown in Figure 5 at wavelengths of λ=0.380μm and λ=0.412μm, which are available for detection of the biomass burring aerosols (Sano et al 2009). From Figure 6 we found that the values of single scattering albedo decrease with the values of imaginary part of refractive index (k), and their differences between λ=0.380μm and λ=0.412μm are little. Neither the phase pattern takes no meaningful variations with respect to Θ and k. However the values for λ=0.380μm are less than those for λ=0.412μm around $\Theta=120^{o}$. This could be available to detect the biomass burning plume.

Figures 7a and 7b represent the distribution of aerosol optical thickness (AOT) at a wave length of 0.55 μm over the Asia on 1st April in 2006 retrieved from Aqua/MODIS data, and simulated with a three-dimensional aerosol-transport–radiation model, SPRINTARS, which is driven by AGCM that was developed by CCSR (Center for Climate System Research), NIES (National Institute for Environmental Studies), and FRCGC (Frontier Research Center for Global Changing), respectively. The numerical scale of AOT (0.55μm) is shown at the bottom of each figure with the gray chart. It is found from both figures in Figure 7 that the values of aerosol optical thickness are higher than 3.0, which exhibits an extreme concentration of aerosols, i.e. aerosol event, over the south-east China. However, the satellite results provide no high values of AOT>5.0 given by model simulations. This fact suggests that retrieval algorithm for aerosol events should be considered more precisely based on the synthetic aspect with the combination of the space-/surface-based measurements, multiple scattering calculations and model simulations.

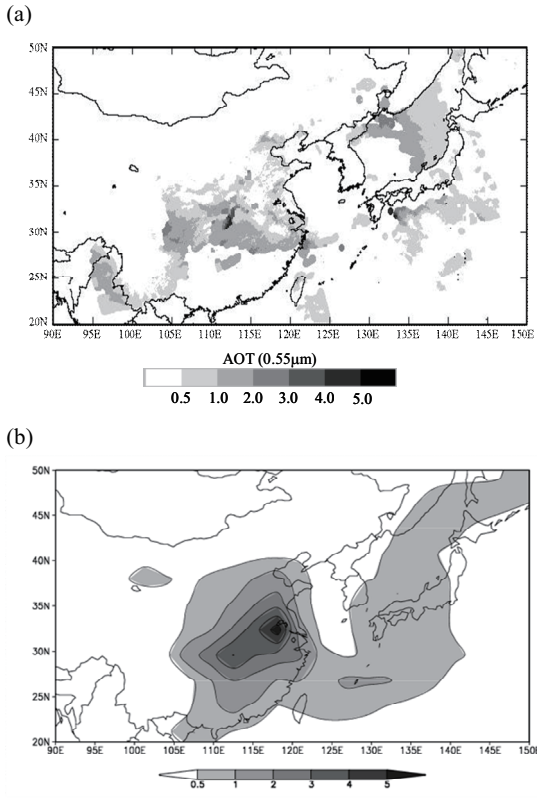

Figure 7 Distribution of aerosol optical thickness (AOT) at a wave length of 0.55 μm over the Asia on 1st April in 2006 retrieved from Aqua/MODIS data (a), and simulated based on a three-dimensional aerosol-transport–radiation model SPRINTARS (b).

REFERENCE

Chandrasekhar,S., 1960. *Radiative transfer*. Dover publications, inc., New York, pp1-54.

Eck, T. F., Holben, B. N., Dubovik, O., Smirnov, A., O'Neill, N. T., Slutsker, I. and Kinne, S.,1999, *Wavelength dependence of the optical depth of biomass burning, urban, and desert dust aerosols,*JGR, 104(D24), pp. 31,333-31,349.

Hansen, .J.E., Travis, L.D., 1974, *Light scattering in planetary atmospheres,* Space Science Reviews 16(4) pp.527-610.

Holben, B.N., Eck, T.F., Slutsker, I., Tanre, D., Buis,J.P., Setzer,A., Vermote,E., Reagan, J.A., Kaufman, Y.J., Nakajima, T., Lavenu, F., Jankowiak, I. and Smirnov A., 1998, *AERONET – A Federated Instrument Network and Data Archive for Aerosol Characterization*, Remote sens.Environ., 66, pp. 1-16.

Mukai(Nakata), M., Nakajima, T., Geophys, J., 2004, A study of long-term trends in mineral dust aerosol distributions in Asia using a general circulation model, Res., 109(D19204),

Mukai, M., Sano, I., Iizuka, T., Yokomae, T. and Mukai, S., 2010 *Detection and Analysis of Dust Aerosol Particles over the East Asia*, J. Remote Sensing Society of Japan, 30(1) pp1-10.

Mukai, S., and Mukai, T,. 1979, Interpretaion of the Infrared Polarization of Venus, ICARUS, 38, 90-99.

Mukai, S., 1990, Atmospheric Correction of Remote Sensing Images of the Ocean Based on Multiple Scattering Calculations, IEEE Transactions on Geoscience and Remote Sensing, 28, pp.696-702.

Sano, I,. Okada, Y., Mukai(Nakata), M. and Mukai, S., 2009. "Retrieval Algorithm Based on Combined Use of

POLDER and GLI for Biomass Aerosols, J. Remote Sensing Society of Japan, 29(1),pp.54-59.

Sano, I., Mukai(Nakata), M., Iguchi, N., and Mukai, S., .2010 ,Suspended Particulate Matter sampling at an urban AERONET site in Japan 2. Relationship between column aerosol optical thickness and $PM_{2.5}$ mass concentration, J. Applied Remote Sensing, 4, pp.403-504.

Uesugi, A. and Irvine,W.M., 1970, Multiple scattering in a plane-parallel atmosphere 1. successive scattering in a semi-infinite medium, Astrophysical Journal, 159, pp127-135.